

# The signal processing of Ultrasonic reflector recognition and tracking technique

Antonin Povolny<sup>1</sup>, Tomonori Ihara<sup>2</sup> and Hiroshige Kikura<sup>1</sup>

<sup>1</sup>Laboratory for Advanced Nuclear Energy, Tokyo Institute of Technology, 2-12-1 Ookayama, Tokyo 152-8550, Japan

<sup>2</sup>Department of Marine Electronics and Mechanical Engineering, Tokyo University of Marine Science and Technology, 2-1-6 Etchujima, Tokyo 135-8533, Japan

Ultrasound Reflector Recognition and Tracking Technique (URRTT) has been developed as a new technique to be applied in the measurement of bubbly two-phase flow. The URRTT measures separately the movement of each reflector, so that the difference in the behaviour of reflectors caused by their size, shape, etc. can be measured. Pulsed ultrasound is emitted into fluid and reflected by objects present in the ultrasound beam volume. The echo signal is recorded by the transducer with a certain delay (transit time) after emission of the original beam. URRTT recognizes reflectors and their positions in the echo signal and tracks reflectors from one pulse's echo to the following ones. The result of URRTT is one-dimensional (in the direction of the ultrasound beam) trajectory of each reflector. Trajectories of reflectors measured simultaneously by other transducers can be added to obtain secondary data such as reflector size, which is very important for measurement of gas bubbles in liquid. This paper focuses on the recognition and tracking algorithms of URRTT. The recognition algorithm uses assumed reflection shape to obtain points corresponding to reflectors' positions. The tracking algorithm connects those points to trajectories. A test experiment shows the performance of URRTT for bubble size measurement.

**Keywords:** Two-phase flow, Trajectory measurement, Signal processing, Tracking, Bubble size measurement

## 1. Introduction

The development of Ultrasonic reflector recognition and tracking technique (URRTT) is motivated by the development of novel simulation techniques for bubbly two-phase flow. While traditional simulation techniques (Two-fluid model) describe all bubbles using one bubble of average parameters to represent them, a technique described in [1] uses many representative bubbles to precisely simulate bubbles of sizes varying from the average. Another approach described in [2] is a direct simulation of phase interface. For further development of those techniques, proper experimental data are required.

Each individual bubble (not just averaged parameters) can be measured using video cameras and video processing. However, cameras require the optical access to the measurement position, which is often impossible due to the pipe wall or due to other bubbles blocking the way. Ultrasound measurement can overcome those limitations. Ultrasound velocity profiler (UVP) was used to measure gas bubble velocity in liquid [3-5]. While UVP provides velocity profiles of gas phase (if it can be distinguished from velocities of other reflectors), it does not distinguish between different bubbles. The attempt to do this by filtering UVP results was presented in [6] along with other methods of detecting phase interface. Simple approach without using UVP has been developed in [7] for single rising bubbles. The signal processing only includes the search for a maximum of amplitude, which corresponds to the position of the bubble surface. The transit time of this peak was recorded for each pulse repetition and then used to construct the trajectory of the bubble. It has been demonstrated that by measuring from opposite sides, bubble size can be measured and that by

parallel measurement at different positions, 2D velocities of bubbles between those two positions can be measured. The accuracy of this approach was investigated in [8]. The main drawback of this technique is that it can be applied only on single bubbles since the separation of bubbles is done only by repetitions with no bubble detected (all amplitudes lower than a threshold value). URRTT has been developed to measure the trajectory of each bubble separately while measuring more bubbles at the same time. To achieve this, completely new approach to signal processing has been applied. The signal processing of URRTT is described in this paper. The connection of trajectories from different measurement positions or directions can provide bubble size or average 2D velocity between different measurement positions. Test measurement of bubble size was performed and its results are presented in this paper to present the performance.

## 2. Measurement configuration

A measurement configuration used for the test measurement is shown in Fig. 1. An ultrasonic transducer (TDX) with 10 mm diameter emits beams into the fluid with bubbles. Second TDX is placed at the same measurement line (opposite direction) to obtain bubble sizes as explained in section 3.3 (Fig. 1 shows another possible configuration, which is not the focus of this paper). Pulses are generated by JapanProbe TIT-10B pulse generator and receiver device and repeated with frequency  $f_{prf} = 2$  kHz. Each pulse is generated by a 1-period long wave of basic frequency  $f_0 = 2$  MHz. The signal is digitised using APX-5040 AD converter (Aval data corp.) at sampling rate 140 MS/s. The AD converter enables simultaneous recording and processing of the data.

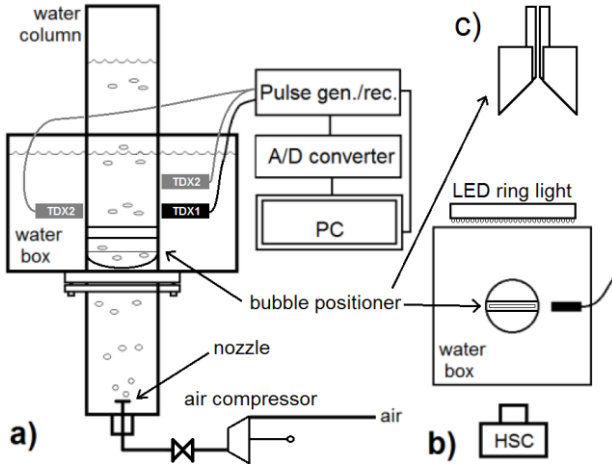


Figure 1: Experimental apparatus. a) front view, b) top view, c) side view on the bubble positioning device.

An acrylic pipe with inner diameter 51.5 mm was used with an acrylic box filled with water to enable observing the flow with a high-speed camera (HSC) Photron Fastcam MAX mounted with Micro-NIKKOR 105mm lens (with  $f/4$ ) positioned in front of the box. A bubble positioning device (with 4 mm wide gap) is placed into the pipe just under the ultrasound beam to bring all the bubbles in the pipe to that beam and to ensure they stay in the 10 mm wide beam long enough to be detected. As a result, higher bubble number density condition was measured without bubble overlapping on the HSC footage. The video is recorded at 2,000 fps with shutter speed  $1/20,000$  s and resolution 1,024 X 256 px. A ring LED light HPR2-150SW (CCS) illuminated the test section from behind. The HSC footage was analysed using the Computer Vision Toolbox of Matlab. The points of each bubble surface closest and furthest from the TDX were tracked in the footage to obtain trajectories of both sides of the bubble surface.

### 3. Signal processing of URRTT

The signal processing has been performed off-line. On-line measurement has not been attempted yet. The whole process is separated into blocks with specific purposes. First, the reflector recognition is performed on each pulse repetition echo signal. It detects all possible positions of reflectors (bubbles) using a reference signal (the assumed shape of the reflection). After that, reflector tracking is performed by joining candidate points from all pulses into chains, which should each represent one reflector. All chains are filtered to avoid noise and checked for erroneous connections of chains from more reflectors into one. Chains represent trajectories of reflector surfaces in the direction of the ultrasound beam. Chains measured by more TDXs for the same reflector (or by TDX and HSC) can be associated with each other. Associated chains can be used to compare data (if connected with HSC) or derive more data such as reflector size or average 2D velocity between two measurement lines.

#### 3.1 Reflector recognition

First, the echo signal is filtered to get rid of any

frequency besides the basic frequency  $f_0$  (during the test measurement, the pass-band was 1-5 MHz). Then, the echo is separated into intervals of width  $1/f_0$  and the absolute value of the signal is summed over each interval to obtain the intensity of that interval. The same summation is done in preparation with no reflectors present in order to determine the background intensity for each interval. If the intensity is greater than the background intensity of the same interval, the interval is a candidate for containing a reflection. Next, cross-correlation is conducted between the reference signal (assumed reflection shape) and a piece of echo belonging to the interval and its close neighbourhood ( $5 \mu\text{s}$  long in this paper). Here, it was assumed that the shape of the reflection is the same as the shape of the propagating pulse and it was measured by a TDX in the opposite direction (the reference signal was  $4 \mu\text{s}$  long in this paper). The time lag  $T$  maximising the cross-correlation is a transit time of the reflector and the maximum itself corresponds to the signal strength. Since the chosen interval length was shorter than the reflection length, only the interval with the highest signal strength (among its neighbours) is chosen to be the candidate point. Each candidate point  $i$  with its time  $t_i$  (pulse emission time), transit time  $T_i$  (reflection delay inside the pulse) and signal strength  $M_i$  is recorded for further processing.

#### 3.2 Reflector tracking

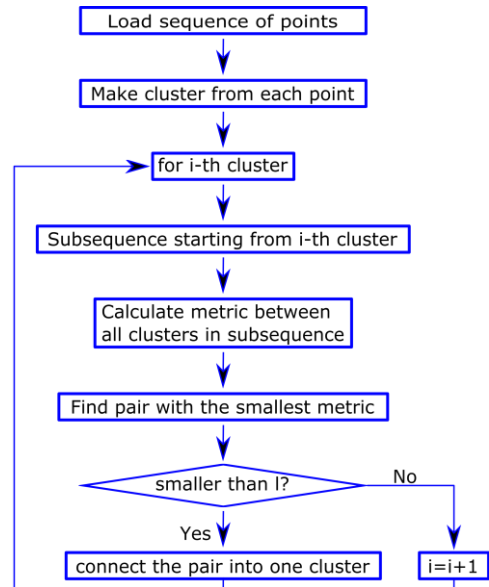


Figure 2: Simplified schematics of the tracking algorithm.

To connect all the points to chains (clusters) representing single reflectors (bubbles), a hierarchical clustering (the agglomerative approach) is employed with a modification for sorted data. All points from reflector recognition are used to create a sequence of singleton clusters sorted by time. The probability that two clusters are caused by the same reflector is described by a specific metric. Two clusters corresponding to the smallest metric value are connected into one cluster in each cycle until the smallest metric is larger than a limiting value  $l$ . The specific flow of the tracking algorithm is illustrated in Fig. 2.

The key point is the definition of the metric. It should measure the likeliness of two clusters being caused by the same bubble. The metric  $D(I, J)$  between clusters  $I$  and  $J$  is calculated from the difference of time and transit time (position) of the last point  $i$  of the earlier cluster  $I$  and the first point  $j$  of the latter cluster  $J$  as

$$D(I, J) = \begin{cases} (t_j - t_i) + w|T_j - T_i| & t_j > t_i \\ l + 1 & t_j \leq t_i \end{cases} \quad (1)$$

where  $w$  is a weighting factor to weigh the importance of differences in time information  $t$  and transit time  $T$  (set to  $w = 200$  in the test measurement). If metric for two clusters is higher than 1, they cannot be connected. The metric is set so that the connection can be done only if each point in the preceding cluster has been recorded earlier than all points in the latter cluster. This condition might seem unnecessary, but it is crucial since it allows keeping all clusters that could connect together and all points inside each cluster sorted by time. This enables to process the large amount of data part-by-part and thus to reduce the computational load (two points with a large difference of time cannot be connected together). It also helps to detect two separate trajectories measured at the same time close from each other. As a result of the algorithm, many chains (clusters) representing reflectors (one chain per reflector) are obtained.

This agglomerative approach works very well if the reflector number density is low. However, for higher reflector number densities, one reflector often follows a previous reflector in a similar track and it is difficult to recognize these two trailing reflectors from a single reflector. Since the signal strength corresponds to the distance between the reflector and the beam axis, each reflector passing through the field will be recorded with a characteristic shape of the signal strength as shown in Fig. 3. This information can be applied to detect trailing reflectors and separate corresponding chains. First, moving average filter is used to smooth the data. Then, peaks of signal strength are detected and they are compared to the minimum values between the peaks. In order to decide whether to separate the chain or not, some requirement (e.g. that both peaks have at least double the signal strength of the minimum) should be set.

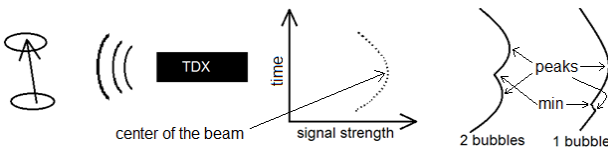


Figure 3: The signal strength corresponds to the distance between the reflector and the beam axis. The signal strength of a passing reflector has a characteristic shape (each point recorded at a different repetition), which can be applied to detect two trailing reflectors.

After a check for trailing reflectors and separation of their corresponding chains, the filter gets rid of the noise. Short chains with few points or with small signal strength are deleted. The transit time  $T$  of each chain can be used

with the speed of sound in water  $c$  to calculate the distance  $x$  between the TDX and the measured bubble surface as

$$x = \frac{Tc}{2} \quad (2)$$

and thus, the chain represents a trajectory of the reflector surface including the signal strength at each point.

### 3.3 Secondary data

The trajectory is a valuable information, but it is too complex to use it directly. Velocity is usually more useful. Instantaneous velocity of reflector surface (towards the TDX) can be easily calculated by taking finite differences of subsequent points of the trajectory and their times.

Results can be statistically described and compared with other measurement or used to validate some code. Comparison reflector-by-reflector is possible if chains measured by URRTT are associated with corresponding trajectories (or other data) from a different source such as HSC. The association is conducted using metric  $B(I, J)$  between two sets of chains ( $I$  is from a different set than  $J$ ) the chain  $I$  contains points from  $i_1$  to  $i_l$  and the chain  $J$  contains points from  $j_1$  to  $j_m$ . The metric is calculated as

$$B(I, J) = |t_{i_1} - t_{j_1}| + |t_{i_l} - t_{j_m}| + \left| \langle t \rangle_{i_1}^{i_l} - \langle t \rangle_{j_1}^{j_m} \right| + w' \left( |x_{i_1} - x_{j_1}| + |x_{i_l} - x_{j_m}| + \left| \langle x \rangle_{i_1}^{i_l} - \langle x \rangle_{j_1}^{j_m} \right| \right) \quad (3)$$

employing time and position from beginning and end of both chains as well as average values. The weight  $w'$  is used to scale between time and space (set to  $w' = 0.1$  s/mm in the test measurement). The metric is calculated for each possible pair of chains and chains are associated with each other starting from the pair corresponding to the lowest metric value (already connected associated chains cannot be associated with some other chain).

It is possible to associate chains of URRTT results from two different TDXs as shown in Fig. 1. Metric  $B(I, J)$  needs to be modified accordingly. In the case of two opposing TDXs, the difference between positions in trajectories is supposed to be  $a$  (assumed reflector size). Terms  $x_i - x_j$  in Eq. 3 need to be replaced with  $x_i - x_j - a$ . For two parallel TDXs at different positions, assumed time delay (needed for the reflector to travel from one TDX to the other one) should be introduced. Once all trajectories are associated, the instantaneous reflector size is obtained from two opposing TDXs (using the known distance between them). For two parallel TDXs at different positions, signal strengths of associated chains can be cross-correlated to obtain the exact time delay needed to travel between those two TDXs. Average 2D velocity can be calculated using this time delay, measured trajectory data and a known distance between axes of those TDXs.

## 4. Example of measurement

An example of air bubble size measurement in water is introduced here. The configuration is described in

section 2 and shown in Fig. 1. Trajectories of opposite bubble surfaces were measured by two opposing TDXs. Transit time/position was measured relative to the opposing inner pipe wall (the transit time of the opposing inner pipe wall was obtained by a cross-correlation with the negative reference signal since water-acrylic boundary reflects in a phase opposite to the water-air bubble surface). The wall-to-wall distance (inner diameter of the pipe) is known, therefore trajectories can be obtained in the same coordinate system and bubble size can be calculated. Results were compared to data obtained from video processing of a HSC footage.

Two cases of measurement are presented here. In both, bubbles were spherical to ellipsoidal shape and bubble size of each bubble was calculated from the HSC footage. The mode of the horizontal size distribution was 4.1 mm and the mode of the vertical size distribution was 2.7 mm. Bubble number density was estimated from the HSC footage as well. In CASE1, the average bubble number density was  $0.44 \text{ ml}^{-1}$  (oscillating from 0 to  $1.57 \text{ ml}^{-1}$ ). At the same time, there were 0 to 8 bubbles in the measurement volume (average 2.27). In CASE2, the average bubble number density was  $0.19 \text{ ml}^{-1}$  (oscillating from 0 to  $0.98 \text{ ml}^{-1}$ ); 0 to 5 bubbles (average 0.98). Instantaneous bubble sizes in the horizontal direction were measured by combining URRTT results of two TDXs. Chains were also associated with HSC results so that bubble-by-bubble comparison of results is possible. For each bubble, average sizes (by URRTT and by HSC) are compared in Fig. 4 and 5. The absolute value of the difference between instantaneous bubble size measured by URRTT and HSC has been averaged over the time interval, where both methods detected the bubble. This value, the normalised bubble size error shows how well does the measurement of instantaneous bubble size agree between HSC and URRTT. Histograms of normalised bubble size errors are shown in Fig. 4 and 5.

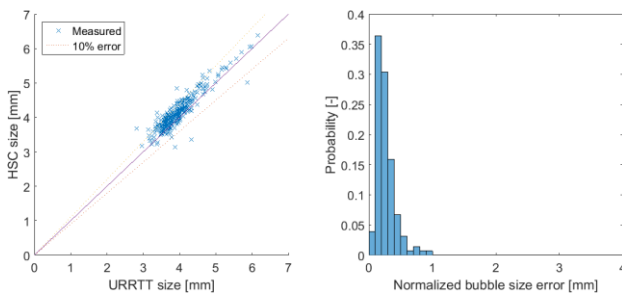


Figure 4: Measurement results for CASE1.

Results show good agreement with HSC values a little bit higher. The difference is around  $200 \mu\text{m}$ , which is comparable with  $60 \mu\text{m}$  pixel resolution of HSC. There are also large uncertainties in the speed of sound obtained from water properties tables using measured temperature of water (speed of sound) and measurement of the inner pipe diameter (needed for calculating the bubble size in URRTT). The video processing algorithm involves the blurred bubble surface image into the bubble region and thus overestimates the bubble size. As such, results show very good agreement, especially for instantaneous bubble

sizes. Higher bubble number in CASE1 lead to a small change of accuracy. However, the reliability of the measurement (ability to detect all the bubbles and avoid erroneous trajectories) decreased.

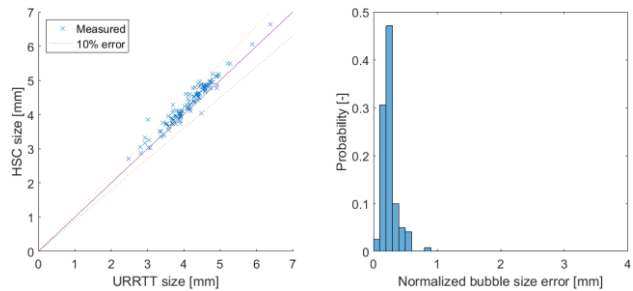


Figure 5: Measurement results for CASE2.

## 5. Summary

The URRTT was developed to measure the trajectory of each bubble crossing the measurement volume. This requires a new approach to signal processing, which was explained in detail. A combined measurement by more TDXs enables to obtain bubble sizes and average bubble velocities between two measurement lines. Presented results show that average bubble sizes measured by URRTT correspond well with the same value from HSC. The difference of  $200 \mu\text{m}$  can be explained by the camera resolution and other measurement uncertainties.

Presented results prove the concept of URRTT as a measurement technique providing a lot of information about the movement of gas bubbles in liquid. As such, it can be applied to measure bubbly flows in many situations where the differences in bubbles sizes are of importance. However, this technique has its limitations. With more bubbles, the reliability of the method is expected to decrease. The evaluation of the range of URRTT application is the subject of future research of authors.

## References

- [1] Krepper E *et al.*: Inhomogeneous MUSIG model - a population balance approach for polydispersed bubbly flows, NURETH-12, Pittsburgh, USA (2007).
- [2] Tryggvason G *et al.*: Direct numerical simulations of gas/liquid multiphase flows, Fluid Dyn. Res., 38-9 (2006), 660-681.
- [3] Aritomi M *et al.*: Measurement system of bubbly flow using Ultrasonic Velocity Profile Monitor and video data processing unit, J. Nucl. Sci. Technol., 33-12 (1996), 915-923.
- [4] Murakawa H *et al.*: Application of ultrasonic Doppler method for bubbly flow measurement using two ultrasonic frequencies, Exp. Therm Fluid Sci., 29-7 (2005), 843-850.
- [5] Murakawa H *et al.*: Application of ultrasonic multi-wave method for two-phase bubbly and slug flows, Flow Meas. Instrum., 19-3 (2008), 205-213.
- [6] Murai Y *et al.*: Ultrasonic detection of moving interfaces in gas-liquid two-phase flow, Flow Meas. Instrum., 21-3 (2010), 356-366.
- [7] Andruszkiewicz A *et al.*: Gas bubble detection in liquid metals by means of the ultrasound transit-time-technique, Eur. Phys. J. Spec. Top., 220 (2013), 53-62.
- [8] Richter T *et al.*: Measuring the diameter of rising gas bubbles by means of the ultrasound transit time technique, Nucl. Eng. Des., 291 (2010), 64-70.